Prophages divert Staphylococcus aureus defenses against host lipids

Biyang Zhou, Amit Pathania, Deepak Pant, David Halpern, Philippe Gaudu, Patrick Trieu Cuot, Andressa Dias-Leao, Charlotte Pagot, Audrey Solgadi, Alexandra Gruss, et al.

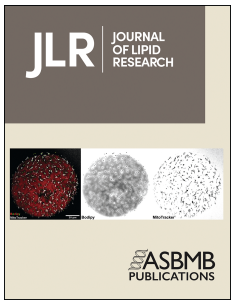

Prophages divert *Staphylococcus aureus* defenses against host lipids

Biyang Zhou, Amit Pathania, Deepak Pant, David Halpern, Philippe Gaudu, Patrick Trieu-Cuot, Andressa Dias-Leao, Charlotte Pagot, Audrey Solgadi, Alexandra Gruss, Karine Gloux

PII: S0022-2275(24)00198-6

DOI: https://doi.org/10.1016/j.jlr.2024.100693

Reference: JLR 100693

To appear in: *Journal of Lipid Research*

Received Date: 3 August 2023

Revised Date: 23 October 2024

Accepted Date: 29 October 2024

Please cite this article as: Zhou B, Pathania A, Pant D, Halpern D, Gaudu P, Trieu-Cuot P, Dias-Leao A, Pagot C, Solgadi A, Gruss A, Gloux K, Prophages divert *Staphylococcus aureus* defenses against host lipids, *Journal of Lipid Research* (2024), doi: https://doi.org/10.1016/j.jlr.2024.100693.

Prophages divert *Staphylococcus aureus* defenses against host lipids

Biyang Zhou [1], Amit Pathania [1], Deepak Pant[1], David Halpern[1], Philippe Gaudu[1], Patrick Trieu-Cuot[3], Andressa Dias-Leao[1], Charlotte Pagot [1], Audrey Solgadi[2], Alexandra Gruss[1], and Karine Gloux[1*]

[1]Université Paris-Saclay, INRAE, AgroParisTech, Micalis Institute, Jouy en Josas, France

[2]UMS-IPSIT SAMM Facility, Université Paris-Saclay, Inserm, CNRS, Ingénierie et Plateformes au Service de l'Innovation Thérapeutique, Paris-Saclay, France

[3]Institut Pasteur, Université Paris Cité, CNRS UMR 2001, Unité de Biologie des Bactéries Pathogènes à Gram-Positif, Paris, France

*Corresponding author

Contact information for corresponding author:

Dr Karine Gloux

Université Paris-Saclay, INRAE, AgroParisTech, Micalis Institute, Jouy en Josas, France

Tel: +33 1 34 65 25 36

Email: karine.gloux@inrae.fr

Short title: Prophages control *S. aureus* fitness in lipids

Abstract

Phages are ubiquitous in bacteria, including clinical *Staphylococcus aureus*, where Sfi 21/Sa3 phages often integrate into the *hlb* gene, which encodes Hlb sphingomyelinase. This integration acts as a rapid regulatory switch for Hlb production. Our findings suggest that Sfi 21/Sa3 prophages and Hlb activity influence *S. aureus* fitness by modulating the incorporation of the toxic linoleic acid (C18:2) from serum into the bacterial membrane. This process relies on C18:2 derived from 1,3-diglyceride, facilitated by the FakB1 kinase subunit. Palmitic acid (C16), primarily released from serum through Hlb activity, competes with C18:2 for FakB1. This mechanism contributes to adaptation to AFN-1252, an antibiotic inhibiting the fatty acid synthesis pathway (anti-FASII). Since *S. aureus* relies on exogenous fatty acids for growth, AFN-1252 treatment leads to increased proportion of C18:2 in the membrane. Furthermore, Hlb inhibition, whether by prophage insertion, gene inactivation, or enzyme inhibition, delays *S. aureus* adaptation, resulting in a higher proportion of C18:2 in the membrane. This study sheds light on the role of lipid environments in infections and may contribute to the accurate prediction of infection risks and therapeutic efficacy. Moreover, since both anti-FASII agent and Hlb inhibitor enhance C18:2 incorporation, they represent potential candidates for combined strategies against *S. aureus.*

Key words:

Fatty acid transport, Phospholipases C, Triglycerides, Sphingolipids, Lipolysis and fatty acid metabolism.

Introduction

Lipids are crucial for bacterial fitness and play a pivotal role in modulating interactions with the host (1-4). However, the impact of environmental lipids on bacterial pathogenesis is often overlooked. Lipids range in complexity from simple short hydrocarbon chains to complex molecules such as triglycerides (TGs), phospholipids (PLs), esterified sterols, and sphingolipids. Fatty acids (FAs), the fundamental building blocks of complex lipids, vary in chain length, side chains, and the number and positions of double bonds. In humans, pathogens encounter diverse lipid environments influenced by genetics and diet, which can correlate infection risk (2,3,5,6). Bacterial lipases break down host-derived lipids into free fatty acids (FAs), which many bacteria can scavenge and incorporate in their membranes (7-12). *Staphylococcus aureus*, a major human pathogen, is particularly adept at incorporating exogenous FAs, such as those found in serum lipids (8,13). Once liberated, these FAs are incorporated into the bacterial membrane through the FakAB system, consisting of FakA (a FA kinase) and the binding proteins FakB1 and FakB2, which prefer saturated and unsaturated FAs, respectively (14-16). Since *S. aureus* lacks desaturase enzymes and cannot synthesize unsaturated FA (17), it relies on external sources for these compounds. The incorporation of monounsaturated (MUFAs) and polyunsaturated FAs (PUFAs) significantly impacts bacterial membrane functions and influences interactions with the host (18-20).

Prophages of the Sfi 21/Sa3 family are the most prevalent phages integrated in staphylococcal genomes, present in over 90% of human clinical isolates (21-25). These prophages have an insertional hotspot in the *hlb* gene (*hlb*-conversion), which encodes the *S. aureus* neutral sphingomyelinase C (Hlb, EC 3.1.4.12, also known as hemolysin B), an enzyme that hydrolyzes sphingomyelins (Fig. 1A) (21,24). The significance of Sfi 21/Sa3 prophages for *S. aureus* adaptation to the human host is attributed to the immune evasion cluster (IEC) encoded by the prophage, as well as to the regulation of Hlb activity (26,27). Sfi 21/Sa3- prophages act as active lysogens, meaning they can excise from the *hlb* gene in response to environmental signals, such as biocides or reactive oxygen species, without killing the bacteria (26,27). The released phage DNA (termed episome) can facilitate rapid adaptation through reinsertion into the same site. Although the roles of sphingomyelinases and IEC in virulence are well studied ((25,28), for review), the impacts of these prophages on *S. aureus* physiology are less understood. Moreover, Sfi

21/Sa3- prophages are implicated in host switching between animals and humans (29,30), making their physiological impact on bacteria crucial for a One Health approach to *S. aureus.*

In this study, we observed that the interruption of the *hlb* gene by the φNM3 prophage (from the Sfi 21/Sa3 family) results in increased incorporation of the bactericidal PUFA linoleic acid (C18:2) into the membrane PLs of *S. aureus*. We investigated the mechanism by which the presence of an *hlb*-converting prophage affects the incorporation of C18:2, which is primarily released from TGs (31). Our findings demonstrate that an intermediate of TG hydrolysis leads to the high incorporation of C18:2 *via* the FakB1 protein subunit. This unexpected binding to FakB1 results in competition with the C16 FA released from sphingomyelins for incorporation into PLs. Furthermore, we showed that inhibition of FASII and/or Hlb activities exacerbates the incorporation and toxicity of C18:2 in PLs, reducing *S. aureus* fitness.

Materials and methods

Bacterial strains.

S. aureus USA300 FPR3757 (methicillin-resistant, referred to as USA300), and the NCTC 8325 derivative strains RN450 and RN450-R, were used in this study (Table 1). RN450, also designated as 8325-4, is a phage-free derivative of the NCTC 8325 strain (32) and has a deficient *fakB1* gene due to a natural deletion. RN450-R is an RN450 derivative in which *fakB1* has been repaired, as described below. Isogenic Newman strains differentiated by the presence of prophages, referred to as WT NM (wild type), TB3 (Δϕ11), TB1 (ΔϕNM3) and TB4 (Δϕ11, ΔϕNM3), were provided by the Schneewind laboratory (Department of Microbiology, University of Chicago). The WT NM has four prophages, including ϕNM3 from the Sfi 21/Sa3 subfamily inserted in *hlb*, and ϕNM4 inserted in the *geh*, which encodes a TG lipase (21). The TB3 strain contains only the *hlb*-converting prophage ϕNM3. The Nebraska USA300 transposon insertion library (University of Nebraska Medical Center) was generously supplied by BEI resources (33). The derivatives used in this work contained insertions, verified by PCR, in the following

genes: *SAUSA300_0320* (*geh*), *SAUSA300_1973* (*hlb*), *SAUSA300_1119* (*fakA*), *SAUSA300_0733* (*fakB1*), *SAUSA300_1318* (*fakB2*). The different strains used in this study, along with their *hlb* and *geh* status (intact or interrupted genes), and prophage insertions, are presented in Table 1.

Construction of an hlb complemented strain

A PCR fragment containing the *hlb* promoter and the open reading frame SACOL_RS10470 (-355 from the ATG start codon and +40 after the TAG stop codon) from the *S. aureus* subsp. *aureus* COL, was cloned between EcoRI and SmaI sites of plasmid pAW8 (34). The primers pairs used for the PCR were 5'-TTGCCGGAATTCTGCAACTTAATTATAGCCAGACTTTC-3' and 5'-CATCAACCCGGGCGTCCTTTTAGAACGAAGCAAG-3'. Genomic coordinates of the 1388 bp cloned segment were 2063371-2064758. This plasmid, named p*hlb*, was used for complementation experiments.

Construction of the RN450-R strain, repaired for fakB1

In the RN450 strain, the *fakB1* gene lacks a 483-bp internal segment. This deletion throughout the entire NCTC 8325 lineage, removing 56% of the 867-bp functional gene (Fig. S1). To repair this deletion, a 1,939-bp DNA fragment containing a functional *fakB1* was amplified to restore the function in RN450, as described for other NCTC 8325 derivatives (35).

Growth media and conditions

Brain heart infusion (BHI) was used as the base medium for *S. aureus* cultures. Bacteria were grown aerobically at 37°C with a starting OD_{600} of 0.02, from 2 to 5-hour precultures prepared in BHI. Mouse or adult bovine serum (Clinisciences, France) was added at 10% final concentration. Stocks of trilinolein (TG18:2, 50 mM), triarachidonin (TG20:4, 10mM), trieicosapentaenoin (TG20:5, 50mM), tridocosahexaenoin (TG22:6, 50mM), 1,2-dilinoleoylglycerol (1,2DG, 50 mM), 1,3-dilinoleoylglycerol (1,3DG, 50 mM), palmitic acid (C16, 100 mM), (Larodan Fine Chemicals, Sweden), orlistat (38 mM, MedChemExpress, France), and the anti-FASII antibiotic AFN-1252 (1 mg/ml, MedChemExpress, France) were prepared in DMSO.

In the absence of an anti-FASII, FA profiles and C18:2 incorporation were determined from bacteria recovered after short growth times (OD_{600} between 1 and 4) to avoid complete consumption of C18:2. Bacterial growth is thus presented as the variation of OD_{600} per hour (OD_{600} /h). To monitor *S. aureus* adaptation to an anti-FASII, bacteria were pre-cultured for 4 hours in BHI medium supplemented with 10% mouse serum (Eurobio, France) and inoculated at OD_{600} 0.02 in the same medium containing 0.5 µg/ml of the anti-FASII AFN-1252. Bacteria were cultured for 17 hours at 37°C in a 96-well microtiter plate using a Spark spectrophotometer (Tecan), with OD_{600} measured every 10 minutes. Growth results are presented as bacterial growth kinetics over time.

Hlb substrate, inducer, and inhibitor

Sphingomyelin was derived from chicken egg yolk (Sigma-Aldrich; St. Louis, MO) and prepared as a 50 mg/ml stock solution in chloroform/methanol (1:1). Hlb sphingomyelinase belongs to the neutral sphingomyelinase family, which requires a lipid-dependent activation by phosphatidylserine. Phosphatidylserine (60 mM, bovine brain, Na salt, Larodan Sweden) was provided in chloroform. GW4869 (Selleckchem.com), a specific inhibitor of the conserved domain of Hlb involved in lipid activation (36,37), was prepared at 1.7 mM in DMSO.

Determination of S. aureus fatty acid profiles

FAs profiles were performed as described previously (9). Briefly, culture aliquots were taken during exponential growth at low OD_{600} (between 1 and 4). After sample preparation, extraction, and trans-esterification of FAs (9), gas chromatography separation was performed by injection of the FA methyl esters in a split-splitless mode on an AutoSystem XL gas chromatograph (Perkin-Elmer) equipped with a ZB-Wax capillary column (30 m x 0.25 mm x 0.25 mm; Phenomenex, France) and a flame ionization detector. FAs were identified based on their retention times and coinjection with purified FA methyl esters standards (Mixture ME100, Larodan, Sweden). Data were recorded and analyzed using a TotalChrom Workstation (Perkin-Elmer). FA peaks were detected between 12 and 40 minutes of elution. Results are shown as representative gas chromatograph profiles or as FA peak areas expressed as a percentage of the total areas of detected peaks.

Detection and characterization of diglycerides, ceramides, and sphingomyelins

Lipid extractions were performed as described by E.G. Bligh and W.J. Dyer (38) with modifications (39). Briefly, freeze-dried supernatants (10ml) of culture (OD_{600} from 3 to 4) were extracted with 9.5 ml of chloroform-methanol 0.3% NaCl (1:2:0.8 v/v/v) at 80°C for 15 min and vortexed for 1 hour at room temperature (RT). After centrifugation at 4,000 rpm for 15 min (RT) supernatants were collected and the debris were re-extracted with 9.5 ml of the same mixture and vortexed for 30 min. After another centrifugation, supernatants were pooled, and 2.5 ml of each chloroform and 0.3% NaCl solutions were added and mixed. Phase separation was achieved by centrifugation at 4,000 rpm for 15 min (RT). The upper phase was discarded, and the chloroform phase was evaporated to dryness under a nitrogen stream and stored at -20°C. Lipids were identified using a previously described method (40). Sphingomyelins and ceramides were identified and characterized by coupling normal phase liquid chromatography with mass spectrometry (NPLC-MS) in negative and positive atmospheric pressure chemical ionization modes (APCI-/+), respectively, with species confirmed by collision induced dissociation MS^2/MS^3 fragmentations (LTQ-Orbitrap Velos Pro). Diglycerides species were determined as illustrated in supplemental data (Fig. S2). Briefly the identification of 1.2- and 1.3- diglycerides was performed from retention times, through comparison with pure diglyceride standards, and the extracted ion current of the main species. Molecular formula of the 1,3-diglycerides, including the number of carbons and the degree of unsaturation were identified by HRMS, LipidMaps database and MS2 fragmentation. Diglycerides were ionized in positive APCI with a loss of water and the addition of a proton $[DG\text{-}H_2O+H]^+$. Lipid spectra were analyzed using Xcalibur™ software (ThermoFisher Scientific, version 4.2.47).

Statistics analysis

Graphs were prepared using Microsoft Excel. Means and standard deviations are presented for culture growth (OD_{600} or OD_{600}/h), FA percentages, and percentages of FA elongated *via* FASII. Statistical significance was determined using unpaired, nonparametric Mann-Whitney tests, as recommended for small sample sizes. For dependent samples, the non-parametric Wilcoxon Signed Rank test was applied.

Results

The hlb-converting prophage ϕNM3 increases C18:2 incorporation from serum into S. aureus phospholipids

Two isogenic Newman strains of *S. aureus*, WT and TB1, differing by the presence of the *hlb*-converting prophage ϕNM3 (Table 1)(41), were grown in control BHI medium. FAs present in their PLs were extracted and analyzed. Both strains exhibited identical FA profiles, corresponding to endogenous FAs produced by FASII activity (Fig. S3), indicating that the ϕNM3 prophage does not affect FAs in membrane PLs in these culture conditions. However, supplementation with 10% mouse serum led to the incorporation of exogenous PUFAs, which *S. aureus* cannot synthesize (17). Notably, only the proportion of C18:2 in PLs was significantly affected by the presence of ϕNM3, showing a two-fold increase in the WT strain compared to TB1 (Fig. 1B). To confirm this observation, we tested adult bovine serum, which contains a broader spectrum of PUFAs, including C18:2, α-linolenic acid (C18:3 ω-3), dihomo-γ-linolenic acid (20:3 ω−6), and arachidonic acid (C20:4 ω-6) (Fig. S4). Since various PUFAs are commonly found in the human body, primarily transported as TGs, we also enriched cultures with different TGs, each containing a single distinct long-chain PUFA commonly found *in vivo*: C18:2, C20:4 ω-6, eicosapentaenoic acid (C20:5 ω-3), or docosahexaenoic acid (C22:6 ω-3). FA profiles of the WT and TB1 strains grown with these PUFAs revealed that only two PUFAs were incorporated into *S. aureus* PLs: C18:2 and, to much lesser extent, C20:4 (Fig. 1C). Furthermore, the presence of ϕNM3 mainly affected C18:2 incorporation (Fig. 1 B & C). Enrichment with 30µM trilinolein (TG18:2 in Fig. 1C), a TG source containing three C18:2 molecules, further increased the proportion of C18:2 in PLs in both strains, indicating that the prophage's effect persisted even with enrichment. Interestingly, enrichment with triarachidonin (TG20:4), a TG source of C20:4, also increased C18:2 incorporation in both strains, even more so than TG18:2 (Fig. 1C). Although the exact mechanism remains unclear, these results suggest that the prophage specifically modulates C18:2 incorporation into *S. aureus* membrane PLs. This effect is

unexpected, as serum sphingomyelins are poor sources of C18:2 (18,42). We therefore questioned how ϕNM3 is linked to C18:2 incorporation into *S.aureus* PLs.

C18:2 from 1,3-dilinoleoylglycerol is highly incorporated and toxic in S. aureus

S. aureus triglyceride lipases can produce both 1,2 and 1,3 diacylglycerol intermediates from TG hydrolysis, as illustrated by the TG18:2 example (Fig. 2A). We analyzed the impact of 1,2-dilinoleoylglycerol (1,2DG) and 1,3-dilinoleoylglycerol (1,3DG) on *S. aureus* growth and their efficiency as substrates for C18:2 incorporation into PLs (Fig. 2B). Since 1,3DG is preferentially released by Geh lipase activity (43,44)(Fig. 2A), the experiment was conducted using the USA300 *geh*$^{+}$ and *geh*$^{-}$ strains (Table 1). We observed that 1,3DG-derived C18:2 was highly incorporated into *S. aureus* PLs at a much higher rate compared to that from 1,2DG (Fig. 2B). Additionally, 1,3DG was significantly more toxic in the *geh*$^{+}$ strain than in the isogenic *geh*$^{-}$ strain (Fig. 2B). However, the resulting proportion of C18:2 and its elongated forms is similar for both strains, suggesting that it is not the determining factor for toxicity. Instead, both the hydrolysis position on the glycerol backbone and the *geh* status are crucial for the toxicity of the released C18:2. We further investigated whether 1,3-diglycerides could be released by *S. aureus* in the presence of serum and whether they contain PUFAs. We used a USA300 *fakA* mutant to block FA incorporation (14) and increase the likelihood of detecting 1,3-diglyceride intermediates. Mass spectrometry with positive APCI ionization detection identified 1,3-diglycerides in the supernatant after growth of the *fakA* mutant in the presence of 10% mouse serum (Fig. 2C, Fig. S2). Orlistat, an inhibitor of Geh activity (45), reduced the levels of both 1,3-diglycerides and the 1,3-diglycerides/1,2-diglycerides ratio in the supernatant (Fig. 2C). Characterization of the 1,3-diglycerides species showed that orlistat also decreased the relative abundance of polyunsaturated 1,3-diglycerides (Fig. 2D, Fig. S2). In conclusion, in the presence of serum, 1,3-diglyceride intermediates are released by bacterial lipases and serve as sources of PUFAs. More than 85% of *S. aureus* isolates are *geh*$^{+}$ (1) and, as a result, may release polyunsaturated 1,3-diglycerides in the presence of serum.

hlb protects S. aureus from 1,3DG-derived C18:2 and promotes C16 incorporation over C18:2.

Although sphingomyelins were not sources of C18:2 in our experiments, we investigated the potential impact of the *hlb* gene on C18:2 incorporation into PLs. To do this, we used the NE1261 strain, a USA300 FPR3757 derivative with an inactive *hlb* gene due to both prophage conversion and transposon insertion, and performed *hlb* complementation. A plasmid carrying an intact *hlb* (p*hlb*) from the *S. aureus* COL strain was constructed and introduced into the NE1261 strain (Table 1). NE1261p*hlb* and the control strain (NE1261pØ, empty plasmid) were grown in BHI supplemented with 10% mouse serum and 10 µM 1,3DG, with or without sphingomyelin (36)(see Material & Methods). Without sphingomyelin supplementation, *hlb* complementation had little to no effect on growth rate. Remarkably, the C18:2 incorporation into PLs was however significantly inhibited (Fig. 3A). Additionally, sphingomyelin supplementation significantly improved growth and led to poor incorporation of C18:2 from 1,3DG into PLs. Surprisingly, *hlb* complementation also significantly inhibited the elongation of both saturated and unsaturated FAs (Fig. 3B). As C18:2 was not transferred into PLs, it may remain in its free form intracellularly, potentially inhibiting the enoyl reductase enzyme (FabI) in FASII, as previously described (31). Since sphingomyelins are potential FA sources (Fig. 3B), we hypothesized that FAs could be released and compete with C18:2 for incorporation into PLs. This would likely involve an intermediate step requiring ceramidase to release such competitive FAs. Although *S. aureus* is not known to produce ceramidase, this enzyme can be present in serum (46). To confirm this, we analyzed sphingomyelin composition and searched for ceramide intermediates in the BHI-mouse serum used for cultures, as well as in the supernatant after the growth of *S. aureus* USA300. Palmitic acid (C16), a common sphingomyelin constituent in human blood (42,47), was identified as the main FA in sphingomyelins under BHI-mouse serum conditions of our first experiment (Fig. 3B). Ceramide intermediates with C16 acyl sources were also found in culture supernatants (Fig. 3B). Furthermore, *hlb*-complementation increased C16 levels in PLs (Fig. 3C). Based on these findings, the effect of the *hlb*-converting prophage on membrane FAs likely reflects an interference between C16 and C18:2 incorporation. We further investigated the underlying mechanism.

Incorporation of 1,3DG-derived C18:2 requires the kinase subunit FakB1 and is inhibited by C16

The substrate selectivity of the Fak kinase complex is determined by the FakB1 and FakB2 FA binding proteins, which are reported to bind saturated and unsaturated FAs, respectively (14-16). We confirmed these phenotypes using the USA300 *fakA*, *fakB1*, and *fakB2* mutants (Table 1) grown in media containing saturated and unsaturated free FAs (Fig. S5). When challenged with TG18:2, the *fakA* mutant did not incorporate C18:2, confirming that phosphorylation is required for the incorporation of C18:2 from TG18:2 into PLs (Fig. S6A). Interestingly, both *fakB1* and *fakB2* mutants failed to show selectivity; both mutants displayed similar capacities to incorporate C18:2 from TG18:2 (Fig. S6A, left). This indicates that while the incorporation of free C18:2 is FakB2-dependent, incorporation from TG18:2 can utilize both FakB proteins.

We further investigated whether the diglycerides released from TG18:2 by *S. aureus* lipases share this FakB binding flexibility. Compared to the TG18:2, incorporation of 1,2DG-derived C18:2 was significantly reduced in the *fakB2* mutant (Fig. S6A, right) aligning with the reported FakB2 binding preference for free unsaturated FAs (14-16). In contrast, incorporation of 1,3DG-derived C18:2 was higher in the *fakB2* mutant than in the *fakB1* mutant (Fig. 4). Moreover, growth of the *fakB1* mutant was strongly impaired compared to the wild-type strain (Fig. 4). These results demonstrate that *fakB1* mediates the incorporation of 1,3DG-derived C18:2 and likely provides protection against the high toxicity of this diglyceride. This unexpected role of *fakB1* suggests a competition with the sphingomyelin-derived C16, a known FakB1 ligand (14). To test this hypothesis, we added C16 in the presence of TG18:2 or 1,3DG. In both the USA300 WT and the *fakB1* mutant strains, the addition of free C16 led to a slight decrease in C18:2 incorporation from TG18:2 or 1,3DG (Fig. 4 and Fig. S6B). In stark contrast, the C16 addition to the *fakB2* mutant (which only has FakB1 available) almost completely halted incorporation of C18:2 from both sources. Since 1,3DG is an intermediate product of TG18:2 hydrolysis, exogenous C16 may compete with 1,3DG-derived C18:2 for binding to FakB1. Interestingly, the protective effect of FakB1 against the 1,3DG was not observed in the presence of C16 (Fig. 4, middle). The presence of C16 may lead to free C18:2, which is toxic to bacteria and inhibits FASII activity (31), consistent with the observed effect of *hlb* on FA elongation (Fig.3A, right). This may represent a form of toxicity not linked to the C18:2

incorporation into PLs. To confirm the direct role of *fakB1* in the incorporation of 1,3DG-derived C18:2, we used the RN450 strain, which carries an in-frame deletion in *fakB1*. This deletion affects two FA binding sites and the phosphotransfer reaction site (Fig. S1), resulting in a non-functional protein. This strain is cured of prophages and carries an intact *hlb* gene (Table 1). We constructed a derivative strain, designed RN450-R, in which *fakB1* is repaired (Table 1). As expected from the above results, 1,3DG-derived C18:2 was more efficiently incorporated by RN450-R than by the *fakB1*-defective RN450 strain (Fig. 5). In RN450, the presence of C16 had no effect on the incorporation of 1,3DG-derived C18:2, likely due to the absence of FakB1. In contrast, C16 strongly inhibited the incorporation of 1,3DG-derived C18:2 in the RN450-R strain (Fig. 5), confirming a direct role of *fakB1* in mediating the competition between 1,3DG-derived C18:2 and C16 for incorporation into PLs. C16 supplementation did not significantly affect the growth of RN450-R, suggesting strain-specific differences in the impact of competition on the toxicity of released C18:2. This strain is a derivative of NCTC8325, which was phage-cured using a two-step UV induction process, resulting in numerous mutations. However, these observations collectively identify *fakB1* as encoding the preferred binding protein for 1,3DG-derived C18:2 and as the key mediator of the competitive incorporation of C18:2 and C16.

Inhibitors of FASII and Hlb increase C18:2 incorporation and limit S. aureus adaptation.

In the presence of an antibiotic targeting FASII (anti-FASII), *S. aureus* adapts by incorporating exogenous FAs, including unsaturated FAs (8). Consequently, bacterial growth becomes exclusively reliant on exogenous FAs under these conditions, likely increasing levels and toxicity of PUFAs in the membrane. We therefore analyzed the potential synergistic effects of inhibiting both FASII and Hlb on *S. aureus* growth. AFN-1252 was used as the FASII inhibitor; this drug targets FASII enoyl reductase enzyme FabI and is effective and safe against skin infections (48,49). GW4869 was used as the sphingomyelinase inhibitor, as it inhibits *S. aureus* sphingomyelinase activation (36,37). Growth of TB3 and TB4 isogenic strains (Table 1) was compared in BHI-mouse serum medium supplemented with 1,3DG, with or without GW4869. When FASII was active, TB3 (*hlb*-converted) exhibited slightly

decreased growth compared to TB4 (intact *hlb*), and GW4869 reversed the growth advantage of TB4 (Fig. 6A, top left). The addition of the FASII inhibitor AFN-1252 significantly slowed growth. As previously reported, *S. aureus* adapted to AFN-1252 in the presence of serum (8) but the TB4 strain displayed a markedly shortened latency period prior to adaptation compared to TB3 (outgrowth <2 hours instead of 12 hours) (Fig. 6A, top right). Furthermore, the addition of GW4869 did not significantly affect TB3 strain growth but delayed that of TB4. These results demonstrate that Hlb activity limits inhibitory effects of AFN1252. We determined FA profiles from these cultures and analyzed the percentage of C18:2 in PLs. AFN-1252 increased the proportion of C18:2 into the PLs of the TB4 strain, especially in the presence of GW4869. We also noticed that AFN-1252 treatment increased the C18:2 percentage fourfold (Fig. 6, bottom), suggesting a synergistic effect on C18:2 toxicity in the *S. aureus* membrane. These results suggest that Hlb activity accelerates adaptation to anti-FASII by limiting C18:2 incorporation and toxicity in the membrane. Safety in humans has been previously demonstrated for both the anti-FASII antibiotic AFN1252 and the Hlb inhibitor GW4869 (48,50), suggesting that they may be good candidates for combinatory strategies against *S. aureus*.

Discussion

This study reveals the crucial role of *hlb*-converting prophages and Hlb sphingomyelinase activity in the lipid metabolism of *S. aureus* and its adaptation to the presence of an anti-FASII agent (Fig. 7). We first demonstrated that Hlb activity unexpectedly inhibits C18:2 incorporation into the bacterial membrane. The link was shown to be the FakB1 kinase subunit: FAs released from TGs and sphingomyelins both compete for this function (Fig. 7A). This mechanism involves a TG-derived 1,3-diglyceride, which promotes significant C18:2 incorporation *via* FakB1 binding, competing with sphingomyelin-derived C16. FakB1's affinity for C18:2, specifically derived from 1,3DG -not free C18:2 or derived from 1,2-diglyceride- remains to be fully understood. The Hlb/C18:2/FakB1connection may represent a natural Achilles' heel exploited by Sfi 21/Sa3 prophages to modulate bacterial fitness in response to the toxicity of this PUFA.

TGs are main constituents of human fat and blood, serving as key circulating reservoirs of C18:2 (51). During infection, both Geh and Hlb lipases are active (27,52). We speculate that C18:2/FakB1 binding and its competition with sphingomyelin-derived C16 may occur *in vivo*. Sfi21/Sa3 are *hlb*-converting prophages that act as regulatory switches for Hlb in most clinical isolates (21-24,27,53). Various stressors, as H_2O_2 or biocides, induce prophage excision into extrachromosomal episomes, allowing rapid phage excision/reinsertion, and control of Hlb activity (23,26). As active lysogens, these prophages may reversibly control the Hlb/C18:2/Fakb1 interaction. This mechanism offers novel insights into the prevalence of *hlb*-converting prophages in clinical isolates and the role of the lipid environment in *S. aureus* adaptation during infection. The incorporation of PUFAs such as C18:2 into PLs alters essential host-interaction functions, including biofilm formation, virulence factor secretion, and interference with immune defense (8,19,20,54-56). Additionally, C18:2 and sphingolipid metabolisms are critical pathways that *S. aureus* manipulates to impair macrophage efficacy (57). Thus, the control of the Hlb/C18:2/FakB1 interaction by *hlb*-converting prophages may play a significant role in *S. aureus* evasion of innate immunity.

The results demonstrate that the levels and balance of TGs and sphingomyelins, along with FA composition and their position in TGs, are crucial factors for *S. aureus* fitness. TGs and sphingomyelins vary based on the state of infection (58,59), the infected site, and individual factors such as diet and genetic makeup (51,58-60). Interestingly, several diseases associated with high risk of infection or severe evolution, such as in Crohn's disease, type 2 diabetes, obesity, and cystic fibrosis, exhibit dysbiosis in TGs and/or sphingomyelins (42,51,57,61-67). Furthermore, novel strategies are particularly needed to combat sepsis (68,69). Lipid emulsions are approved or under investigation for intravenous nutrition in sepsis patients ((https://clinicaltrials.gov/study/NCT03405870)(70)). The mechanism connecting TGs and SMs open new hypotheses and potential future lipid formulations for prevention or to counter fatal outcomes.

This study also shows that *hlb*-conversion limits adaptation to anti-FASII treatment (mechanistic model in Fig. 7A). In line with the Hlb/C18:2/FakB1 connection, the absence of Hlb activity increases the incorporation of toxic C18:2 and delays adaptation to anti-FASII treatment. What can be inferred from

previous *in vivo* studies of anti-FASII adaptation? *S. aureus* was shown to adapt efficiently to anti-FASII treatment in a mouse model (8). Since Hlb activity occurs during infection (for review (25)), we propose that prophage excision contributes to anti-FASII adaptation *in vivo*. Membrane fatty acid composition is known to affect the efficacy of other antibiotics, such as daptomycin and vancomycin (71,72), making the Hlb/C18:2/FakB1 connection relevant for future drug screening and development. Furthermore, inhibitors of FASII or Hlb increase the proportion of C18:2 in membrane PLs. Thus, combining an Hlb inhibitor or anti-FASII treatment with TG18:2 enrichment could have a synergistic effect against *S. aureus*. A strategy incorporating this natural lipid-based mechanism may reduce drug dosages and lower the risk of resistant variant emergence. In conclusion, the mechanism by which these prophages alter *S. aureus* lipid metabolism is crucial for addressing challenges in infection prevention and healthcare.

Data availability

This article contains supplemental data. All data supporting the findings of this study are available within this article and its supplemental data.

Acknowledgment

We thank Myriam Gominet (Institut Pasteur) for the construction of the *S. aureus* RN450 *fakB1*-repaired strain. We are grateful to members of the MicrobAdapt team for stimulating discussion of this work.

CRediT author statement

K. G., B. Z., A. P., D. P., C.P., A. DL., P. G., and D.H. investigation; K. G., A. G., A. P., P. G., and P. T-C. writing-review & editing; K.G., A. G., A. P., A. S. and P. T-C. methodology; K. G. conceptualization, validation, formal analysis, writing original draft, visualization, supervision, project administration. K. G. & A.G. funding acquisition and resources.

Funding sources

This work was supported by French granting agencies: French Agence Nationale de la Recherche (StaphEscape project ANR-16-CE15-0013), the Fondation pour la Recherche Medicale (DBF20161136769), and the INRAE's department MICA (LipStaph project).

Conflict of interest

The authors declare that they have no conflicts of interest with the contents of this article.

Abbreviations

FA: fatty acid; FakAB, kinase module including the FakA FA kinase, and FakB binding proteins; IEC, immune evasion cluster; Hlb or SMase, hemolysin B or sphingomyelinase C; orli, orlistat; PL, phospholipid; PUFA, polyunsaturated fatty acid; SM, sphingomyelin; TG, triglyceride; TG18:2, trilinolein; TG20:4, triarachidonine; TG20:5, trieicosapentaenoin; TG22:6, tridocosahexaenoin; 1,2DG, 1,2-dilinoleoylglycerol; 1,3DG, 1,3-dilinoleoylglycerol.

References

1. Chen, X. and Alonzo, F., 3rd. (2019) Bacterial lipolysis of immune-activating ligands promotes evasion of innate defenses. *Proc. Natl. Acad. Sci. USA.* **116**, 3764-3773
2. Sun, H., Zhang, X., Shi, W. and Fang, B. (2019) Association of soft tissue infection in the extremity with glucose and lipid metabolism and inflammatory factors. *Exp. Ther. Med.* **17**, 2535-2540
3. Trinder, M., Boyd, J.H. and Brunham, L.R. (2019) Molecular regulation of plasma lipid levels during systemic inflammation and sepsis. *Curr. Opin. Lipidol.* **30**, 108-116
4. Gajenthra Kumar, N., Contaifer, D., Jr., Baker, P.R., Ekroos, K., Jefferson, K.K. and Wijesinghe, D.S. (2018) Untargeted lipidomic analysis to broadly characterize the effects of pathogenic and non-pathogenic staphylococci on mammalian lipids. *PloS one*, **13**, e0206606
5. Feingold, K.R. and Grunfeld, C. (2000) In Feingold, K. R., Anawalt, B., Boyce, A., Chrousos, G., Dungan, K., Grossman, A., Hershman, J. M., Kaltsas, G., Koch, C., Kopp, P. *et al.* (eds.), *Endotext*, South Dartmouth (MA)
6. Kaysen, G.A., Ye, X., Raimann, J.G., Wang, Y., Topping, A., Usvyat, L.A., *et al.* (2018) Lipid levels are inversely associated with infectious and all-cause mortality: international MONDO study results. *J. Lipid. Res.* **59**, 1519-1528
7. Gloux, K., Guillemet, M., Soler, C., Morvan, C., Halpern, D., Pourcel, C., *et al.* (2017) Clinical relevance of type II fatty acid synthesis bypass in *Staphylococcus aureus*. *Antimicrob. Agents Chemother.* **61**, e02515-02516
8. Kenanian, G., Morvan, C., Weckel, A., Pathania, A., Anba-Mondoloni, J., Halpern, D., *et al.* (2019) Permissive fatty acid Incorporation promotes staphylococcal adaptation to FASII antibiotics in host environments. *Cell Rep.* **29**, 3974-3982 e3974
9. Morvan, C., Halpern, D., Kenanian, G., Hays, C., Anba-Mondoloni, J., Brinster, S. *et al.* (2016) Environmental fatty acids enable emergence of infectious *Staphylococcus aureus* resistant to FASII-targeted antimicrobials. *Nat. Commun.* **7**, 12944.

10. Morvan, C., Halpern, D., Kenanian, G., Pathania, A., Anba-Mondoloni, J., Lamberet, G., *et al.* (2017) The *Staphylococcus aureus* FASII bypass escape route from FASII inhibitors. *Biochimie*. **141**, 40-46

11. Brinster, S., Lamberet, G., Staels, B., Trieu-Cuot, P., Gruss, A. and Poyart, C. (2009) Type II fatty acid synthesis is not a suitable antibiotic target for Gram-positive pathogens. *Nature*. **458**, 83-86.

12. Hays, C., Lambert, C., Brinster, S., Lamberet, G., du Merle, L., Gloux, K., *et al.* (2021) Type II fatty acid synthesis pathway and cyclopropane ring formation are dispensable during *Enterococcus faecalis* systemic infection. *J. Bacteriol.* **203**, e0022121

13. Delekta, P.C., Shook, J.C., Lydic, T.A., Mulks, M.H. and Hammer, N.D. (2018) *Staphylococcus aureus* utilizes host-derived lipoprotein particles as sources of fatty acids. *J. Bacteriol.* **200**, (11):e00728-00717

14. Parsons, J.B., Broussard, T.C., Bose, J.L., Rosch, J.W., Jackson, P., Subramanian, C. *et al.* (2014) Identification of a two-component fatty acid kinase responsible for host fatty acid incorporation by *Staphylococcus aureus*. *Proc. Natl. Acad. Sci. U S A.* **111**, 10532-10537

15. Broussard, T.C., Miller, D.J., Jackson, P., Nourse, A., White, S.W. and Rock, C.O. (2016) Biochemical roles for conserved residues in the bacterial fatty acid-binding protein family. *J. Biol. Chem.* **291**, 6292-6303

16. Cuypers, M.G., Subramanian, C., Gullett, J.M., Frank, M.W., White, S.W. and Rock, C.O. (2019) Acyl-chain selectivity and physiological roles of *Staphylococcus aureus* fatty acid-binding proteins. *J. Biol. Chem.* **294**, 38-49

17. Parsons, J.B., Frank, M.W., Jackson, P., Subramanian, C. and Rock, C.O. (2014) Incorporation of extracellular fatty acids by a fatty acid kinase-dependent pathway in *Staphylococcus aureus*. *Mol. Microbiol.* **92**, 234-245

18. Hines, K.M., Alvarado, G., Chen, X., Gatto, C., Pokorny, A., Alonzo, F., 3rd, *et al.* (2020) Lipidomic and ultrastructural characterization of the cell envelope of *Staphylococcus aureus* grown in the presence of human serum. *mSphere*. **5**(3), e00339-20

19. Nguyen, M.T., Hanzelmann, D., Hartner, T., Peschel, A. and Gotz, F. (2016) Skin-specific unsaturated fatty acids boost the *Staphylococcus aureus* innate immune response. *Infect. Immun.* **84**, 205-215

20. Arsic, B., Zhu, Y., Heinrichs, D.E. and McGavin, M.J. (2012) Induction of the staphylococcal proteolytic cascade by antimicrobial fatty acids in community acquired methicillin resistant *Staphylococcus aureus*. *PloS one*. **7**, e45952

21. Goerke, C., Pantucek, R., Holtfreter, S., Schulte, B., Zink, M., Grumann, D., *et al.* (2009) Diversity of prophages in dominant *Staphylococcus aureus* clonal lineages. *J. Bacteriol.* **191**, 3462-3468

22. Verkaik, N.J., Benard, M., Boelens, H.A., de Vogel, C.P., Nouwen, J.L., Verbrugh, H.A., *et al.* (2011) Immune evasion cluster-positive bacteriophages are highly prevalent among human *Staphylococcus aureus* strains, but they are not essential in the first stages of nasal colonization. *Clin. Microbiol. Infect*. **17**, 343-348

23. Goerke, C., Wirtz, C., Fluckiger, U. and Wolz, C. (2006) Extensive phage dynamics in *Staphylococcus aureus* contributes to adaptation to the human host during infection. *Mol. Microbiol*. **61**, 1673-1685

24. van Wamel, W.J., Rooijakkers, S.H., Ruyken, M., van Kessel, K.P. and van Strijp, J.A. (2006) The innate immune modulators staphylococcal complement inhibitor and chemotaxis inhibitory protein of *Staphylococcus aureus* are located on beta-hemolysin-converting bacteriophages. *J. Bacteriol.* **188**, 1310-1315

25. Rohmer, C. and Wolz, C. (2021) The role of *hlb*-converting bacteriophages in *Staphylococcus aureus* host adaption. *Microb. Physiol.* **31**, 109-122

26. Deutsch, D.R., Utter, B., Verratti, K.J., Sichtig, H., Tallon, L.J. and Fischetti, V.A. (2018) Extra-chromosomal DNA sequencing reveals episomal prophages capable of impacting virulence factor expression in *Staphylococcus aureus*. *Front. Microbiol.* **9**, 1406

27. Tran, P.M., Feiss, M., Kinney, K.J. and Salgado-Pabon, W. (2019) phiSa3mw prophage as a molecular regulatory switch of *Staphylococcus aureus* beta-toxin production. *J. Bacteriol.* **201**, e00766-00718

28. Flores-Diaz, M., Monturiol-Gross, L., Naylor, C., Alape-Giron, A. and Flieger, A. (2016) Bacterial sphingomyelinases and phospholipases as virulence factors. *Microbiol. Mol. Biol. Rev.* **80**, 597-628

29. Rohmer, C., Dobritz, R., Tuncbilek-Dere, D., Lehmann, E., Gerlach, D., George, S.E., Bae, T., Nieselt, K. and Wolz, C. (2022) Influence of *Staphylococcus aureus* strain background on Sa3int phage life cycle switches. *Viruses*. **14**. 2471

30. Chaguza, C., Smith, J.T., Bruce, S.A., Gibson, R., Martin, I.W. and Andam, C.P. (2022) Prophage-encoded immune evasion factors are critical for Staphylococcus aureus host infection, switching, and adaptation. *Cell Genom.* **2**. 100194

31. Zheng, C.J., Yoo, J.S., Lee, T.G., Cho, H.Y., Kim, Y.H. and Kim, W.G. (2005) Fatty acid synthesis is a target for antibacterial activity of unsaturated fatty acids. *FEBS Lett.* **579**, 5157-5162

32. Herbert, S., Ziebandt, A.K., Ohlsen, K., Schafer, T., Hecker, M., Albrecht, D., *et al*. (2010) Repair of global regulators in *Staphylococcus aureus* 8325 and comparative analysis with other clinical isolates. *Infect. Immun.* **78**, 2877-2889

33. Fey, P.D., Endres, J.L., Yajjala, V.K., Widhelm, T.J., Boissy, R.J., Bose, J.L. *et al.* (2013) A genetic resource for rapid and comprehensive phenotype screening of nonessential *Staphylococcus aureus* genes. *mBio*. **4**, e00537-00512

34. Katayama, Y., Zhang, H.Z., Hong, D. and Chambers, H.F. (2003) Jumping the barrier to beta-lactam resistance in *Staphylococcus aureus*. *J. Bacteriol.* **185**, 5465-5472

35. Pathania, A., Anba-Mondoloni, J., Gominet, M., Halpern, D., Dairou, J., Dupont, L., *et al.* (2021) (p)ppGpp/GTP and malonyl-CoA modulate *Staphylococcus aureus* adaptation to FASII antibiotics and provide a basis for synergistic bi-therapy. *mBio*. **12**, e03193-03120

36. Airola, M.V., Shanbhogue, P., Shamseddine, A.A., Guja, K.E., Senkal, C.E., Maini, R., *et al.* (2017) Structure of human nSMase2 reveals an interdomain allosteric activation mechanism for ceramide generation. *Proc. Nat. Acad. Sci. USA*. **114**, E5549-E5558

37. Luberto, C., Hassler, D.F., Signorelli, P., Okamoto, Y., Sawai, H., Boros, E., *et al.* (2002) Inhibition of tumor necrosis factor-induced cell death in MCF7 by a novel inhibitor of neutral sphingomyelinase. *J. Biol. Chem.* **277**, 41128-41139

38. Bligh, E.G. and Dyer, W.J. (1959) A rapid method of total lipid extraction and purification. *Can. J. Biochem. Physiol*. **37**, 911-91

39. Thedieck, K., Hain, T., Mohamed, W., Tindall, B.J., Nimtz, M., Chakraborty, T., *et al.* (2006) The MprF protein is required for lysinylation of phospholipids in listerial membranes and confers resistance to cationic antimicrobial peptides (CAMPs) on Listeria monocytogenes. *Mol. Microbiol.* **62**, 1325-1339

40. Abreu, S., Solgadi, A. and Chaminade, P. (2017) Optimization of normal phase chromatographic conditions for lipid analysis and comparison of associated detection techniques. *J. Chromatogr. A*, **1514**, 54-7

41. Bae, T., Baba, T., Hiramatsu, K. and Schneewind, O. (2006) Prophages of *Staphylococcus aureus* Newman and their contribution to virulence. *Mol. Microbiol.* **62**, 1035-1047

42. Hanamatsu, H., Ohnishi, S., Sakai, S., Yuyama, K., Mitsutake, S., Takeda, *et al.* (2014) Altered levels of serum sphingomyelin and ceramide containing distinct acyl chains in young obese adults. *Nutr. Diabetes*, **4**, e141

43. Douchet, I., De Haas, G. and Verger, R. (2003) Lipase regio- and stereoselectivities toward three enantiomeric pairs of didecanoyl-deoxyamino-O methyl glycerol: a kinetic study by the monomolecular film technique. *Chirality*. **15**, 220-226

44. Horchani, H., Ben Salem, N., Chaari, A., Sayari, A., Gargouri, Y. and Verger, R. (2010) Staphylococcal lipases stereoselectively hydrolyse the sn-2 position of monomolecular films of diglyceride analogs. Application to sn-2 hydrolysis of triolein. *J. Colloid. Interface Sci.* **347**, 301-308

45. Kitadokoro, K., Tanaka, M., Hikima, T., Okuno, Y., Yamamoto, M. and Kamitani, S. (2020) Crystal structure of pathogenic *Staphylococcus aureus* lipase complex with the anti-obesity drug orlistat. *Sci. Rep.* **10**, 5469

46. Jiang, Y., He, X., Simonaro, C.M., Yi, B. and Schuchman, E.H. (2021) Acid ceramidase protects against hepatic ischemia/reperfusion injury by modulating sphingolipid metabolism and reducing inflammation and oxidative stress. *Front. Cell Dev. Biol.* **9**, 633657

47. Hammad, S.M., Pierce, J.S., Soodavar, F., Smith, K.J., Al Gadban, M.M., Rembiesa, B., *et al.* (2010) Blood sphingolipidomics in healthy humans: impact of sample collection methodology. *J. Lipid Res.* **51**, 3074-3087

48. Hafkin, B., Kaplan, N. and Murphy, B. (2015) Efficacy and safety of AFN-1252, the first *Staphylococcu*s-specific antibacterial agent, in the treatment of acute bacterial skin and skin structure infections, including those in patients with significant comorbidities. *Antimicrob. Agents Chemother*. **60**, 1695-1701

49. Kaplan, N., Albert, M., Awrey, D., Bardouniotis, E., Berman, J., Clarke, T., *et al.* (2012) Mode of action, in vitro activity, and in vivo efficacy of AFN-1252, a selective antistaphylococcal FabI inhibitor. *Antimicrob. Agents Chemother*. **56**, 5865-5874

50. Essandoh, K., Yang, L., Wang, X., Huang, W., Qin, D., Hao, J., Wang, Y., Zingarelli, B., Peng, T. and Fan, G.C. (2015) Blockade of exosome generation with GW4869 dampens the sepsis-induced inflammation and cardiac dysfunction. *Biochim. Biophys. Acta*, **1852**, 2362-2371

51. Hodson, L., Skeaff, C.M. and Fielding, B.A. (2008) Fatty acid composition of adipose tissue and blood in humans and its use as a biomarker of dietary intake. *Prog. Lipid. Res.* **47**, 348-380

52. Hu, C., Xiong, N., Zhang, Y., Rayner, S. and Chen, S. (2012) Functional characterization of lipase in the pathogenesis of *Staphylococcus aureus*. *Biochem. Biophys. Res. Commun*. **419**, 617-620

53. Feiner, R., Argov, T., Rabinovich, L., Sigal, N., Borovok, I. and Herskovits, A.A. (2015) A new perspective on lysogeny: prophages as active regulatory switches of bacteria. *Nat. Rev. Microbiol*. **13**, 641-650

54. Lopez, M.S., Tan, I.S., Yan, D., Kang, J., McCreary, M., Modrusan, Z., *et al.* (2017) Host-derived fatty acids activate type VII secretion in *Staphylococcus aureus*. *Proc. Natl. Acad. Sci. U S A.* **114**, 11223-11228

55. DeMars, Z.R., Krute, C.N., Ridder, M.J., Gilchrist, A.K., Menjivar, C. and Bose, J.L. (2021) Fatty acids can inhibit *Staphylococcus aureus* SaeS activity at the membrane independent of alterations in respiration. *Mol. Microbiol.* **116**, 1378-1391

56. Lee, J.H., Kim, Y.G. and Lee, J. (2022) Inhibition of *Staphylococcus aureus* biofilm formation and virulence factor production by petroselinic acid and other unsaturated C18 fatty acids. *Microbiol. Spectr*. **10**, e0133022

57. Al-Daghri, N.M., Torretta, E., Barbacini, P., Asare, H., Ricci, C., Capitanio, D., *et al.* (2019) Sphingolipid serum profiling in vitamin D deficient and dyslipidemic obese dimorphic adults. *Sci. Rep*. **9**, 16664

58. Yan, B., Fung, K., Ye, S., Lai, P.M., Wei, Y.X., Sze, K.H., *et al.* (2022) Linoleic acid metabolism activation in macrophages promotes the clearing of intracellular *Staphylococcus aureus*. *Chem. Sci*.**13**, 12445-12460

59. Bravo-Santano, N., Ellis, J.K., Calle, Y., Keun, H.C., Behrends, V. and Letek, M. (2019) Intracellular *Staphylococcus aureus* elicits the production of host very long-chain saturated fatty acids with antimicrobial activity. *Metabolites*. **9**(7):148

60. Astorg, P., Bertrais, S., Laporte, F., Arnault, N., Estaquio, C., Galan, P., *et al.* (2008) Plasma n-6 and n-3 polyunsaturated fatty acids as biomarkers of their dietary intakes: a cross-sectional study within a cohort of middle-aged French men and women. *Eur. J. Clin. Nutr.* **62**, 1155-1161

61. Trinder, M., Walley, K.R., Boyd, J.H. and Brunham, L.R. (2020) Causal inference for genetically determined levels of high-density lipoprotein cholesterol and risk of infectious disease. *Arterioscler. Thromb. Vasc. Biol.* **40**, 267-278

62. Wheelock, C.E. and Strandvik, B. (2020) Abnormal n-6 fatty acid metabolism in cystic fibrosis contributes to pulmonary symptoms. *Prostaglandins Leukot. Essent. Fatty Acids*. **160**, 102156

63. Guerrera, I.C., Astarita, G., Jais, J.P., Sands, D., Nowakowska, A., Colas, J., *et al.* (2009) A novel lipidomic strategy reveals plasma phospholipid signatures associated with respiratory disease severity in cystic fibrosis patients. *PloS one*. **4**, e7735

64. Ferru-Clement, R., Boucher, G., Forest, A., Bouchard, B., Bitton, A., Lesage, S., *et al.* (2023) Serum lipidomic screen identifies key metabolites, pathways, and disease classifiers in Crohn's disease. *Inflamm. Bowel Dis*. **29**, 1024-1037

65. Scoville, E.A., Allaman, M.M., Adams, D.W., Motley, A.K., Peyton, S.C., Ferguson, S.L., *et al.* (2019) Serum polyunsaturated fatty acids correlate with serum cytokines and clinical disease activity in Crohn's disease. *Sci. Rep*. **9**, 2882

66. Imamura, S., Morioka, T., Yamazaki, Y., Numaguchi, R., Urata, H., Motoyama, K., *et al.* (2014) Plasma polyunsaturated fatty acid profile and delta-5 desaturase activity are altered in patients with type 2 diabetes. *Metabolism*. **63**, 1432-1438

67. Zhong, X., Xiao, C., Wang, R., Deng, Y., Du, T., Li, W., *et al.* (2024) Lipidomics based on UHPLC/Q-TOF-MS to characterize lipid metabolic profiling in patients with newly diagnosed type 2 diabetes mellitus with dyslipidemia. *Heliyon*. **10**, e26326

68. Amunugama, K., Pike, D.P. and Ford, D.A. (2021) The lipid biology of sepsis. *J. Lipid Res.* **62**, 100090

69. Mu, A., Klare, W.P., Baines, S.L., Ignatius Pang, C.N., Guerillot, R., Harbison-Price, N., *et al.* (2023) Integrative omics identifies conserved and pathogen-specific responses of sepsis-causing bacteria. *Nat. Commun.***14**, 1530

70. Kulkarni, A.V., Anand, L., Vyas, A.K., Premkumar, M., Choudhury, A.K., Trehanpati, N., *et al.* (2021) Omega-3 fatty acid lipid emulsions are safe and effective in reducing endotoxemia and sepsis in acute-on-chronic liver failure: An open-label randomized controlled trial. *J. Gastroenterol. Hepatol.* **36**, 1953-1961

71. Boudjemaa, R., Cabriel, C., Dubois-Brissonnet, F., Bourg, N., Dupuis, G., Gruss, A., *et al.* (2018) Impact of bacterial membrane fatty acid composition on the failure of daptomycin to kill *Staphylococcus aureus*. *Antimicrob. Agents Chemother*. **62**(7):e00023-18

72. Sidders, A.E., Kedziora, K.M., Arts, M., Daniel, J.M., de Benedetti, S., Beam, J.E., *et al.* (2023) Antibiotic-induced accumulation of lipid II synergizes with antimicrobial fatty acids to eradicate bacterial populations. *eLife*. **12**:e80246.

73. Diep, B.A., Gill, S.R., Chang, R.F., Phan, T.H., Chen, J.H., Davidson, M.G., *et al.* (2006) Complete genome sequence of USA300, an epidemic clone of community-acquired meticillin-resistant *Staphylococcus aureus*. *Lancet.* **367**, 731-739

74. McCarthy, A.J., Witney, A.A. and Lindsay, J.A. (2012) *Staphylococcus aureus* temperate bacteriophage: carriage and horizontal gene transfer is lineage associated. *Front. Cell Infect. Microbiol*. **2**, 6

Table title:

Table 1. Strains and phages.

Figure Titles:

Figure 1. *hlb*-converting prophage enhances C18:2 incorporation from serum and triglycerides (TGs). (A) The insertion site of phage ϕNM3 in the *hlb* gene, which encodes the enzyme sphingomyelinase Hlb, results in a truncation at the enzyme's N-terminus at position 56 of the 330 amino acid sequence. The gene *map* encodes an extracellular adherence protein of broad specificity (Eap/Map)*;* and the gene *lukF* encodes a protein from the leukocidin/hemolysin toxin family. (B) The *hlb*-conversion increases the incorporation of linoleic acid (C18:2) from mouse serum. The wild type Newman strain (WT NM), containing the *hlb*-converting ϕNM3 prophage, and the TB1 strain, lacking ϕNM3 and having an intact *hlb* gene, were grown for 2 hours in BHI medium supplemented with 10% mouse serum. FAs were extracted from PLs and analyzed by gas chromatography. On the left, representative FA profiles are shown with y-axis representing the relative FA abundance (mV response) at indicated peak positions. Endogenously produced FAs are in black, while FAs not synthesized by *S. aureus* but incorporated from serum are in purple. On the right, histograms depict the relative amounts of C18:2 incorporated into PLs. (C) The *hlb*-conversion specifically affects the incorporation of C18:2 from TGs into PLs. The WT NM and TB1 strains were cultured in BHI medium supplemented with 10% bovine serum and enriched with 30µM of triarachidonin (TG20:4), trieicosapentaenoin (C20:5) or tridocosahexaenoin (C22:6). Data are presented as mean +/- standard deviation from independent experiments (n=4 for (A), n=3 for (B)). Statistical significance was determined using the Mann Whitney test for incorporated FAs. **, $p \leq 0.01$.

Figure 2. Crucial role of 1,3-diglycerides in C18:2 toxicity in *S. aureus*. (A). The non-selective cleavage of TGs by *S. aureus* Geh activity results in both 1,2- and 1,3- diglycerides (1,2DG and 1,3DG from TG18:2). Most lipases preferentially cleave at position 1, releasing 1,2-diglycerides, as illustrated for 1,2DG from TG18:2. In contrast, Geh can cleave at both positions, thus releasing 1,3-diglycerides (42,

43). (B) The 1,3DG supplementation results in a high incorporation of C18:2 into PLs**.** WT NM (*geh*::tn) and TB3 (intact *geh*) strains were cultured for 2 hours in BHI medium supplemented with 10 µM of either 1,2DG or 1,3DG. The relative amounts of incorporated C18:2 (C18:2 and its elongated forms) were determined as in Figure 1B and are presented as FAs derived from the diglycerides. Notably, C18:2 was more efficiently incorporated and toxic when derived from 1,3DG compared to 1,2DG, with TB3 (intact *geh*) showing extreme sensitivity. (C) *S. aureus* lipase generates 1,3-diglycerides. The USA300 *fakB1*::tn mutant was cultured in BHI medium with 10% mouse serum, with or without 30µM orlistat, a TG lipase Geh inhibitor. Lipids present in the supernatant were extracted and analyzed using normal phase liquid chromatography (NPLC) coupled to high resolution mass-spectrometry (HRMS). 1,2 and 1,3 diglycerides were identified by their retention times and through comparison with pure diglyceride standards (Fig. S2). (D) The 1,3-diglycerides generated by *S. aureus* lipase contain polyunsaturated FAs. The 1,3-diglycerides with polyunsaturation (formulas in red) and generated in (C) were identified by HRMS. They are ionized in positive APCI with a loss of water and the addition of a proton $[DG\text{-}H_2O+H]^+$ (Fig. S2). Data are presented as mean +/- standard deviation from independent experiments (n=4 for (B), n=3 for (C)). Statistical significance was determined by the Mann Whitney test in (B) and by the non-parametric Wilcoxon Signed Rank test in (C). **, $p \leq 0.01$. ***, $p \leq 0.001$.

Figure 3. Plasmid-driven expression of *hlb* affects *S. aureus* fitness, inhibits FASII, and increases C16 in PLs. (A) The *hlb*-complementation protects from 1,3DG-derived C18:2 incorporation and toxicity but inhibits FA elongation. The NE1261 mutant (Tn insertion in *hlb*), carrying either an empty plasmid (p∅) or a plasmid with an intact *hlb* (p*hlb*) was grown for 3 hours in BHI medium supplemented with 10% mouse serum and 10 µM 1,3DG. Activated sphingomyelin (SM, 200 µM) was added as an Hlb substrate. Left: Growth is presented as the OD_{600} increase per hour. Middle: Incorporation of C18:2 and its elongated form C20:2 in PLs. Relative amounts of incorporated FAs were determined as in Figure 2B and expressed in a percentage of total FAs. Right: FA elongation by FASII was determined from the relative amounts of elongated forms of C16, C18, C18:1 and C18:2, and expressed as a percentage of total (FA + elongated) for each. (B) Sphingomyelins and ceramides from *S. aureus* culture supernatants are sources of C16. The USA300 strain was cultured in BHI medium in the presence of 10% mouse serum. Lipids were extracted,

and sphingomyelins and ceramides were identified and characterized by NPLC-MS in negative and positive atmospheric pressure chemical ionization mode, respectively, with species confirmed by MS^2 and MS^3. Left: The main sphingomyelin species deduced from NPLC and subsequent fragmentations is SM(d18:1/16:0). The detection threshold of SM species was around 0.025 mg/mL. Traces of SM(d18:1/18:1) and SM(d18:1/18:0) were detected but no source of C18:2. Middle and Right: Ceramide intermediates containing C16 were detected in culture supernatants: a dihydroceramide (Cer(d18:1,O2/16:0)), and a hexylceramides (HexCer(d18:1,O2/16:0)). (C) Plasmid-driven expression of *hlb* increases C16 incorporation from sphingomyelin. Cultured of NE1261 p∅ and p*hlb* strains were analyzed for FAs content as in described in (A). Total C16 incorporated in PLs was determined as for C18:2 in Fig. 1B and expressed as percentage of total FAs. Data presented in histograms are means +/- standard deviations from independent experiments (n=3). Statistical significance was determined by the Mann-Whitney in (A) and (C). **, $p \leq 0.01$, *$p \leq 0.05$.

Figure 4. FakB1 mediates the incorporation of 1,3DG-derived C18:2, competing with C16 incorporation. USA300 (WT), *fakB1::tn*, and *fakB2::tn* mutant strains were cultured for 2 hours in BHI medium supplemented with 10 µM 1,3DG, with or without 20 µM C16. FA profiles were analyzed as described in Figure 1B. Bacterial growth and incorporated C18:2 were measured as in Figure 3A. In the FA profiles, purple arrows indicate C18:2 and its elongated forms (C20:2 and C22:2). Growth is presented as OD_{600} per hour (OD/h). Data in histograms are means +/- standard deviations from independent experiments (n=5). Statistical significance was determined by the Mann-Whitney test for C18:2 incorporation and for OD_{600}/h.**, $p \leq 0.01$; *, $p \leq 0.05$.

Figure 5. Restoration of *fakB1* enhances incorporation of 1,3DG-derived C18:2 and competition with C16. RN450 (*fakB1*$^-$) and RN450-R (*fakB1*$^+$) strains were cultured for 3 hours in BHI medium supplemented with 10 µM 1,3DG, with or without 40 µM C16. FA profiles were determined as described in Figure 1B. Bacterial growth and incorporated C18:2 were measured as described in Figure 3A. In the FA profiles, purple arrows indicate C18:2 and elongated forms (C20:2 and C22:2). Growth is presented

as OD_{600} per hour (OD_{600}/h). Data in histograms are means +/- standard deviations from independent experiments (n=5). Statistical significance was determined using the Mann-Whitney test for C18:2 incorporation and OD_{600}/h.**, $p \leq 0.01$.

Figure 6. Hlb activity and anti-FASII treatments enhance C18:2 incorporation in *S. aureus* PLs. TB3 (ϕNM3 in *hlb*) and TB4 (no phage) strains were cultured in BHI medium supplemented with 10% mouse serum, 30 µM 1,3DG, and with or without 50µM GW4869 (an inhibitor of Hlb activity). Top left: bacterial growth rates in the absence of anti-FASII treatment, performed in glass tubes. Top right: growth kinetics in the presence of 0.5µg/ml AFN-1252 (a FASII inhibitor), measured in 96-well microtiter plates with OD600 reading every 10 minutes. Bottom: C18:2 incorporation with or without AFN-1252. C18:2 incorporation was determined in the TB4 and TB3 strains as described in Figure 2B. Data are means +/- standard deviations from independent experiments (n=4). Statistical significance was determined by the Mann-Whitney test for on OD_{600}/h and by the Wilcoxon Signed Rank test for incorporated C18:2; *, $p \leq 0.05$. n.s: not significant.

Figure 7. Mechanistic model of C18:2 toxicity in *S. aureus* and its enhancement by an inhibition of FASII or sphingomyelinase activity.

(A) Modulation of C18:2 incorporation by the *hlb*-converting prophage is based on FA competition for FakB1. The model highlights three major features: 1) The 1,3-diglyceride intermediate, released by *S. aureus* Geh lipase, leads to increased incorporation and toxicity of C18:2 in the *S. aureus* membrane. 2) C18:2 derived from 1,3-diglycerides binds to FakB1 for incorporation into PLs, in contrast to free C18:2 or that derived from 1,2-diglycerides. 3) Hlb activity contributes to the release sphingomyelin-derived C16, which competes for FakB1 and prevents the binding and incorporation of C18:2 into PLs. Unbound C18:2 inhibits FASII (31) and hinders FA elongation and bacterial growth. As an active lysogen, the phage exerts rapid control over Hlb activity (23,26). Depending to the environmental Hlb substrates, it modulates bacterial adaptation to the highly toxic C18:2 derived from 1,3-diglycerides.

(B) Blocking FASII or sphingomyelinase activity exacerbates C18:2 incorporation, leading to reduced bacterial adaptation. Under anti-FASII conditions, S *aureus* relies on exogenous FAs for growth (8), such

as C18:2, which is incorporated into membrane PLs and is toxic. Furthermore, inhibiting Hlb activity reduces competition for FakB1 binding, allowing greater incorporation of C18:2 into PLs (see Fig. 7A). Therefore, inhibitors of both FASII and Hlb are potential combinatory drugs that could enhance the natural defense mechanism involving C18:2.

SM: sphingomyelin, TG-C18:2: triglyceride containing C18:2, 1,3 diglyceride-C18:2: 1,3-diglyceride containing C18:2.

Supplemental data

Supplementary Figure S1. FakB1 defect in the RN450 strain. Alignment of FakB1 sequences from Newman and NCTC 8325 strains. The NCTC 8325 lineage, which includes the RN450 strain, carries an in-frame deletion in *fakB1* (a 483-bp within the 867-bp intact *fakB1* gene). The non-deleted region of NCTC 8325 FakB1 shares 100% identity with the corresponding region in the Newman strain. Blue arrows indicate amino acids required for FA binding and FakA-mediated phosphotransfer (1).

1. Cuypers M.G., Subramanian C., Gullett J.M., Frank M.W., White S.W., Rock C.O. (2019) Acyl-chain selectivity and physiological roles of *Staphylococcus aureus* fatty acid-binding proteins. *J Biol Chem.* **294**(1):38-49

Supplementary Figure S2. Structural identification of 1,3 and 1,2 diglycerides using LC-HRMS and collision induced dissociation (CID) fragmention. (A) Extracted ion chromatograms of: a) m/z 551.503, DG 32:0, dipalmitin commercial standard from Sigma-Aldrich; b) m/z 577.517, DG 34:1 in the presence of the *fakA* mutant; c) m/z 577.517, DG 34:1 in the presence of the *fakA* mutant and orlistat. The 1,3 and 1,2 diglycerides have different retention times (1) but very similar MS2 spectra. (B) Examples of 1,3 and 1,2 diglycerides MS2 CID fragmentation spectra with a collision energy of 35% and fatty acid composition identification (2): a) m/z 551.50 MS2 corresponding to commercial standard DG 16:0-16:0; b) m/z 577.52 MS2 from culture with the *fakA* mutant leading to DG 16:0-18:1; c) m/z 577.52 MS2 from culture with the *fakA* mutant in the presence of orlistat leading to DG 16:0-18:1. (C) Diglyceride identification based on retention time, HRMS positive ionization (positive APCI with a loss of water and the addition of a proton $[DG\text{-}H_2O+H]^+$), LipidMaps database (3) and MS2 fragmentation.

nd: not determined.

1. Abreu, S., Solgadi, A. and Chaminade, P. (2017) Optimization of normal phase chromatographic conditions for lipid analysis and comparison of associated detection techniques. J. Chromatogr. A, 1514, 54-7.

2. Murphy, R. C. (2014) Tandem Mass Spectrometry of Lipids; Robert C Murphy.doi.org/10.1039/9781782626350.

3. http://www.lipidmaps.org

Supplementary Figure S3. Fatty acid profiles of *S. aureus* cultured in BHI medium are not affected by the prophage status. Four isogenic Newman strains, either lysogenized or not by prophages (ϕNM1, ϕNM2, ϕNM3, ϕNM4) as shown, were cultured in BHI. FAs were extracted and analyzed as described in Fig. 1B. Representative FA profiles and means of FA relative amounts (in purple) from three independent experiments are shown. Statistical significance was determined by the Kruskal-Wallis test to compare the FA compositions between the four strains. Profiles were not significantly different, p value> 0.05.

Supplementary Figure S4. Fatty acid profile from adult bovine serum. A representative profile, determined as in Figure 1B is shown. This serum contains different PUFAs: linoleic acid (C18:2), α-linolenic acid (C18:3 ω-3), dihomo-γ-linolenic acid (20:3 ω−6), and arachidonic acid (C20:4 ω-6).

Supplementary Figure S5. Phenotype validation of *fakA, fakB1* and *fakB2* mutants. The USA300 wild type (WT) and mutant strains were cultured in BHI medium in the presence of exogenous FAs. Total membrane FAs were extracted, analysed, and presented as in Fig. 1B. (A) FAs profiles from the WT strain and the *fak* mutants cultured in the presence of an FA cocktail (free C14:0, C16:0, and C18:1, 0.17 mM each). The three exogenous FAs and their elongated forms are indicated in blue. The orange arrow indicates C18:1 elongation into C20:1. Blue crosses indicate that *fakA* is essential for FA incorporation and *fakB2* is essential for C18:1 incorporation. Purple arrows indicate that *fakB1* is involved in the incorporation of C14 and C16. (B) *fakB2* is required for the incorporation of free C18:2. The WT strain and the *fakB2*::tn mutant were cultured in the presence 10µM free C18:2. Left: FA profiles, C18:2 and its elongated forms are represented in blue. Right: C18:2 incorporation into PLs. Note that free C18:2 is

poorly incorporated in the *fakB2* mutant compared to the WT. Data presented are means +/- standard deviations from independent experiments (n=3). Statistical significance was determined by the Mann-Whitney test. *, $p \leq 0.05$.

Supplementary Figure S6. Roles of *fak* genes in the incorporation of C18:2 from TG18:2 or 1,2DG. Experiments and FAs profiles were performed as described in Figure 4, except that the USA300 WT and *fak* mutant strains (Table 1) were cultured in the presence of 30µM TG18:2 or 1,2DG, as sources of C18:2. (A) Representative FA profiles from *fakA*, *fakB1* and *fakB2* mutants cultured in the presence of TG18:2 or 1,2DG. Left: The *fakA* defective strain fails to incorporate C18:2 from TG18:2, while both *fakB1* and *fakB2* mediate incorporation of TG18:2-derived C18:2. Right: The *fakB2* gene, and not *fakB1*, affects C18:2 incorporation from 1,2 dilinolein (1,2DG). (B) C16 inhibits the incorporation of C18:2 from TG18:2 through competition for FakB1. The *fakB2* mutant (encoding only *fakB1*) fails to incorporate TG18:2-derived C18:2 in the presence of C16. Growth rates presented as OD_{600} per hour suggest that FakB1 protects against C18:2 toxicity and that C16 inhibits growth when only FakB1 is active by releasing free C18:2 in *S. aureus*. TG18:2-derived C18:2 and its elongated forms are indicated in blue, and blue crosses indicating their absence. Purple arrows indicate a C16 increase due to exogenous supply. Blue arrows indicate the inhibition of TG18:2-derived C18:2 and its elongated forms. Profiles are representative of independent experiments (n=3). Histograms are means +/- standard deviations from these experiments. Statistical significance was determined by the Mann-Whitney test.; *, $p \leq 0.05$.

Table 1. Strains and phages

Strains	Designation	*hlb* interruption	*fakAB* defect	*geh* interruption	Ref
Wild types					
NM	Newman	yes;by ϕNM3	no	yes by φNM4	(41)
USA300	USA300_FPR3757	yes;by ϕSa3USA300	no	no	(73)
RN450	RN0450	no	yes; deleted region	no	(32)
Impact of Hlb and Geh lipases					
TB1	Newman-derived ΔϕNM3	no	no	yes by φNM4 prophage	(41)
TB3	Newman-derived ΔϕNM1.2.4	yes;by ϕNM3	no	no	(41)
TB4	Newman-derived ΔϕNM1.2.4ΔϕNM3	no	no	no	(41)
NE1261	USA300-derived *hlb*::tn	yes; by ϕSa3USA300 and Tn	no	no	(74)
NE1261p∅	USA300-derived *hlb*::tn pAW8	yes; by ϕSa3USA300 and Tn	no	no	this study
NE1261p*hlb*	USA300-derived *hlb*::tn pAW8*hlb*	yes; by ϕSa3USA300 and Tn	no	no	this study
NE1775	USA300-derived *geh*::tn	yes; by ϕSa3USA300	no	yes; by Tn	(74)
Role of the FakAB system in C18:2 toxicity					
USA300*fakA*	USA300-derived NE229	yes; by ϕNM3	yes; *fakA* interrupted by Tn	no	(74)
USA300*fakB1*	USA300-derived NE1540	yes; by ϕNM3	yes; *fakB1* interrupted by Tn	no	(33)
USA300*fakB2*	USA300-derived NE403	yes; by ϕNM3	yes; *fakB2* interrupted by Tn	no	(33)
RN450-R	RN0450-R	no	no; repaired for *fakB1*	no	this study

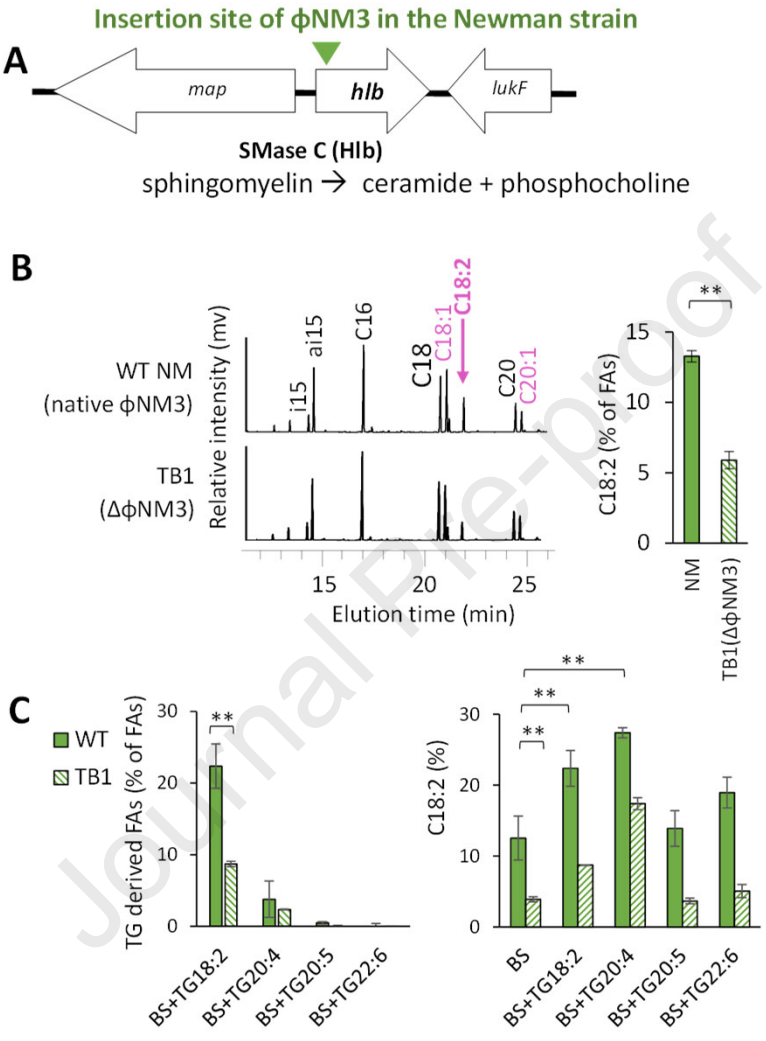
Insertion site of ϕNM3 in the Newman strain
A
map
hlb
lukF
SMase C (Hlb)
sphingomyelin → ceramide + phosphocholine
B
WT NM
(native ϕNM3)
TB1
(ΔϕNM3)
Relative intensity (mv)
i15
ai15
C16
C18
C18:1
C18:2
C20
C20:1
15
20
25
Elution time (min)
C18:2 (% of FAs)
**
NM
TB1(ΔϕNM3)
C
WT
TB1
TG derived FAs (% of FAs)
BS+TG18:2
BS+TG20:4
BS+TG20:5
BS+TG22:6
C18:2 (%)
BS

Fig. 1

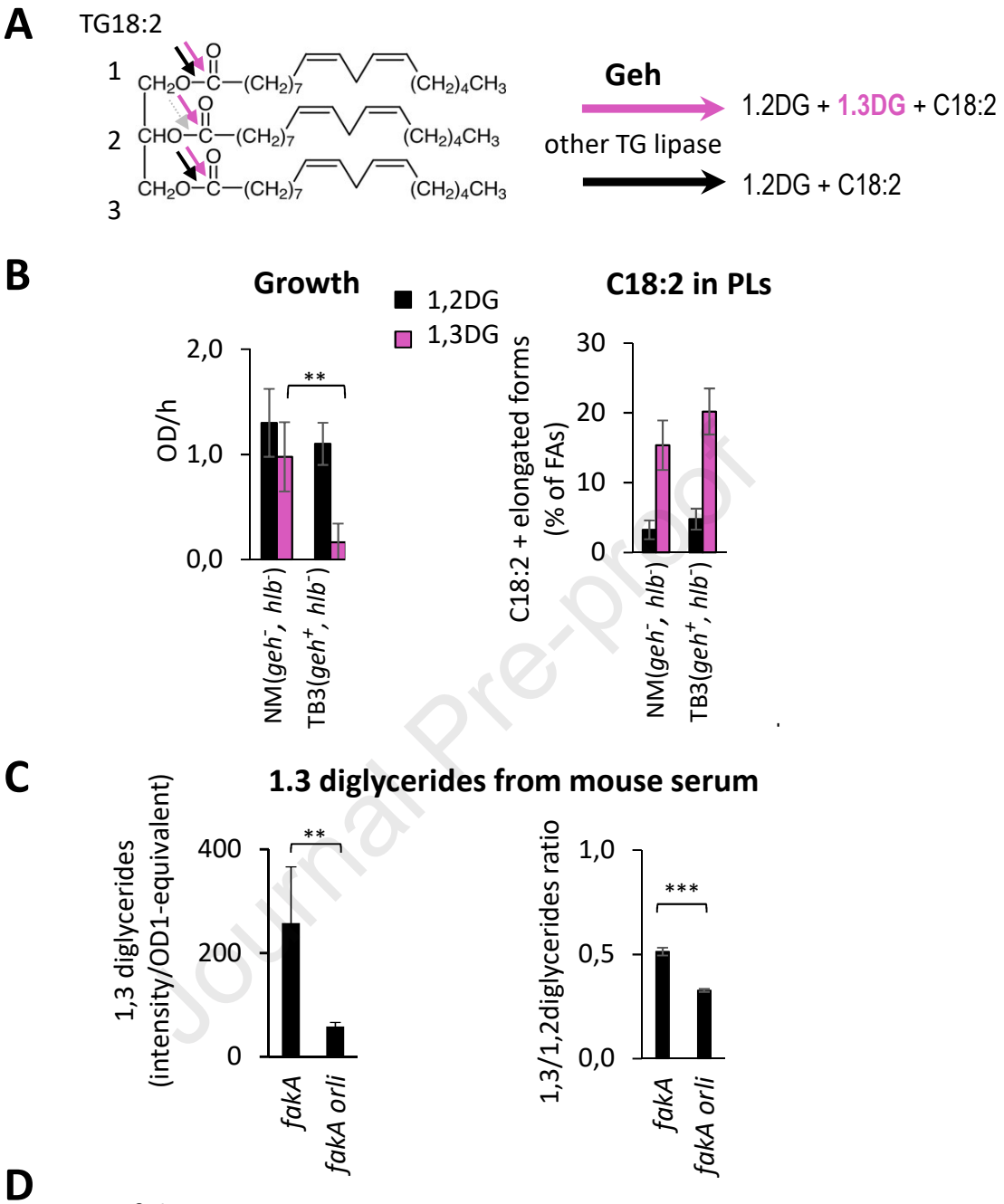

Lipids with unsaturated FAs

m/z [DG-H_2O+H]$^+$	Corresponding species	Neutral formula
575.498	DG 34:2	C37H68O5
577.514	DG 34:1	C37H70O5
597.485	DG 36:5	C39H66O5
599.498	DG 36:4	C39H68O5
601.514	DG 36:3	C39H70O5
603.529	DG 36:2	C39H72O5

Fig. 2

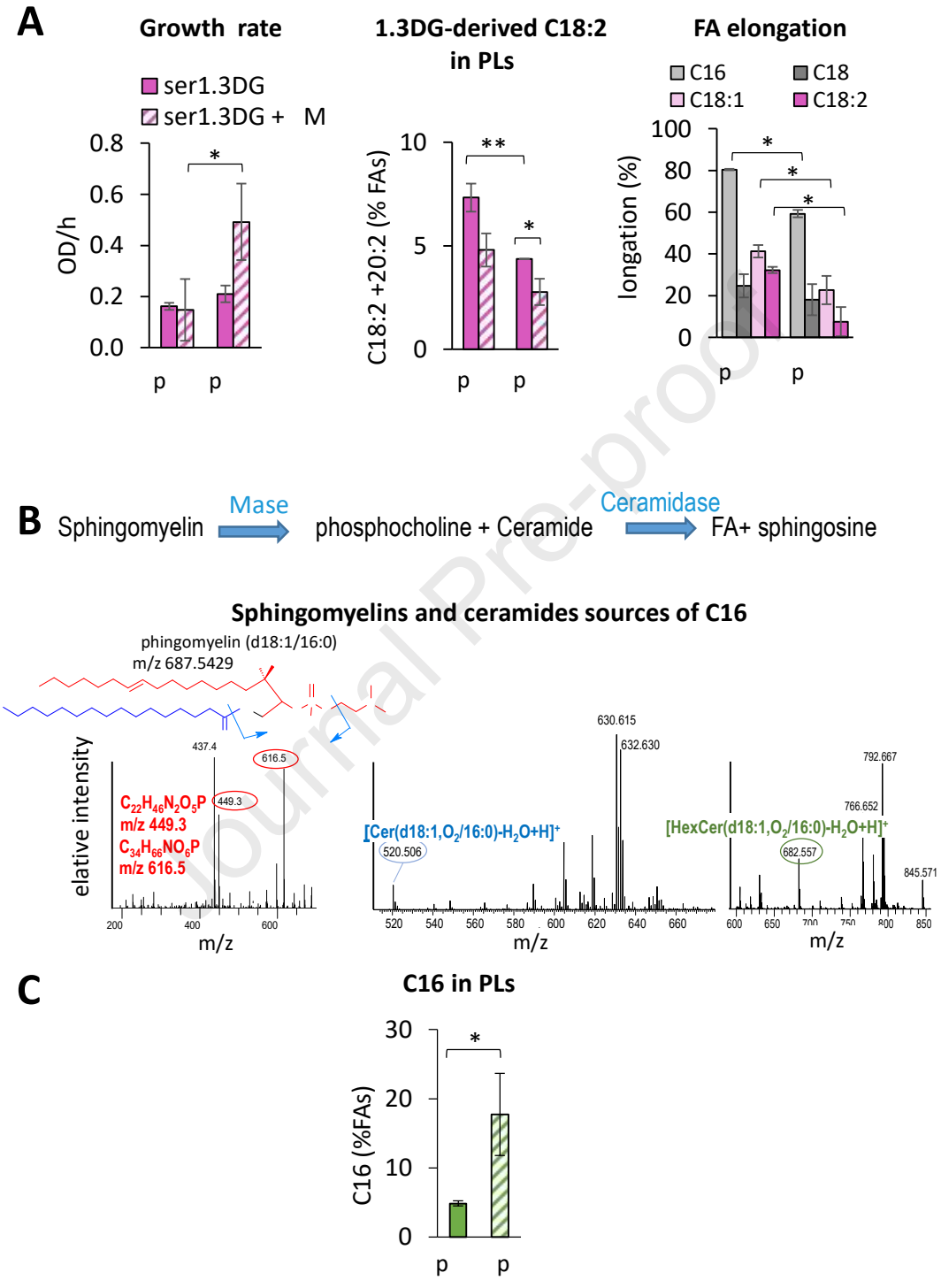
A
Growth rate
ser1.3DG
ser1.3DG + M
OD/h
0.8
0.6
0.4
0.2
0.0
*
p
p
1.3DG-derived C18:2 in PLs
C18:2 +20:2 (% FAs)
10
5
0
**
*
p
p
FA elongation
C16
C18
C18:1
C18:2
longation (%)
100
80
60
40
20
0
*
*
*
p
p
B
Sphingomyelin
Mase
phosphocholine + Ceramide
Ceramidase
FA+ sphingosine
Sphingomyelins and ceramides sources of C16
phingomyelin (d18:1/16:0)
m/z 687.5429
elative intensity
437.4
616.5
449.3
C22H46N2O5P
m/z 449.3
C34H66NO6P
m/z 616.5
200
400
600
m/z
630.615
632.630
[Cer(d18:1,O2/16:0)-H2O+H]+
520.506
520
540
560
580
600
620
640
660
m/z
792.667
766.652
[HexCer(d18:1,O2/16:0)-H2O+H]+
682.557
845.571
600
650
850
m/z
C
C16 in PLs
C16 (%FAs)
30
20
10
0
*
p
p

Fig. 3

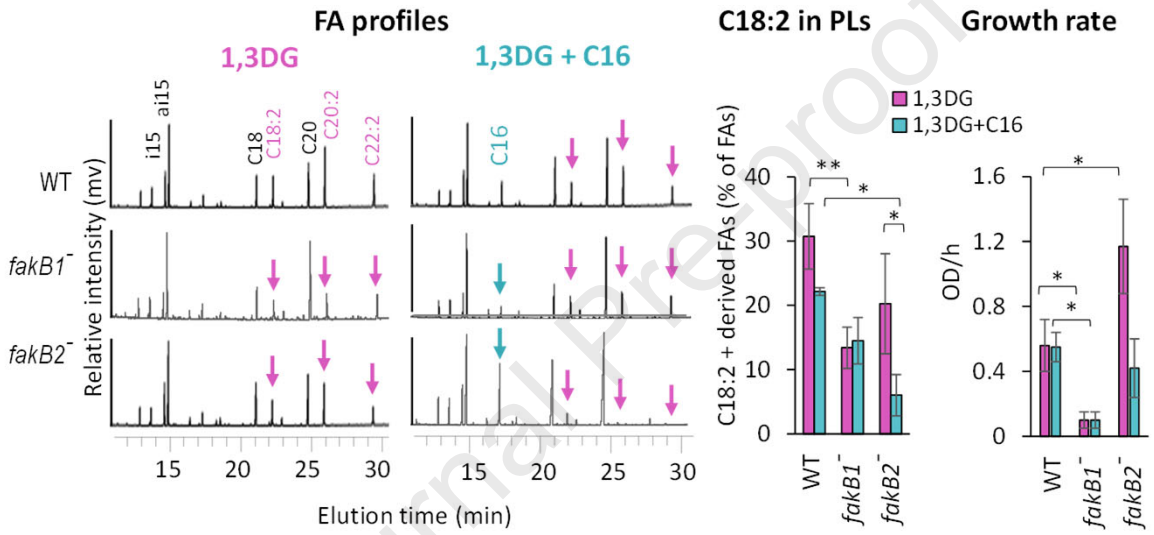

Fig. 4

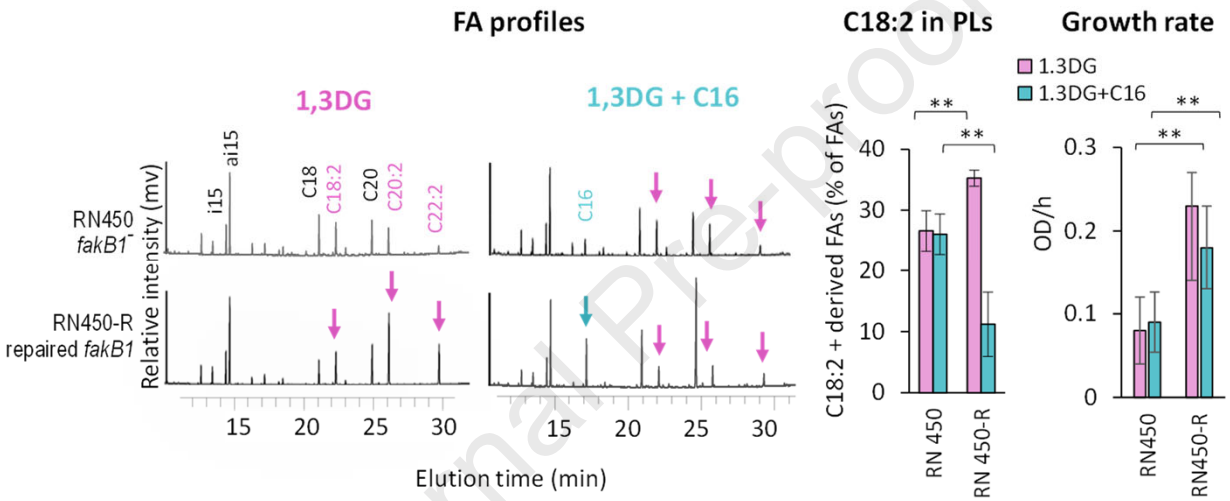

Fig. 5

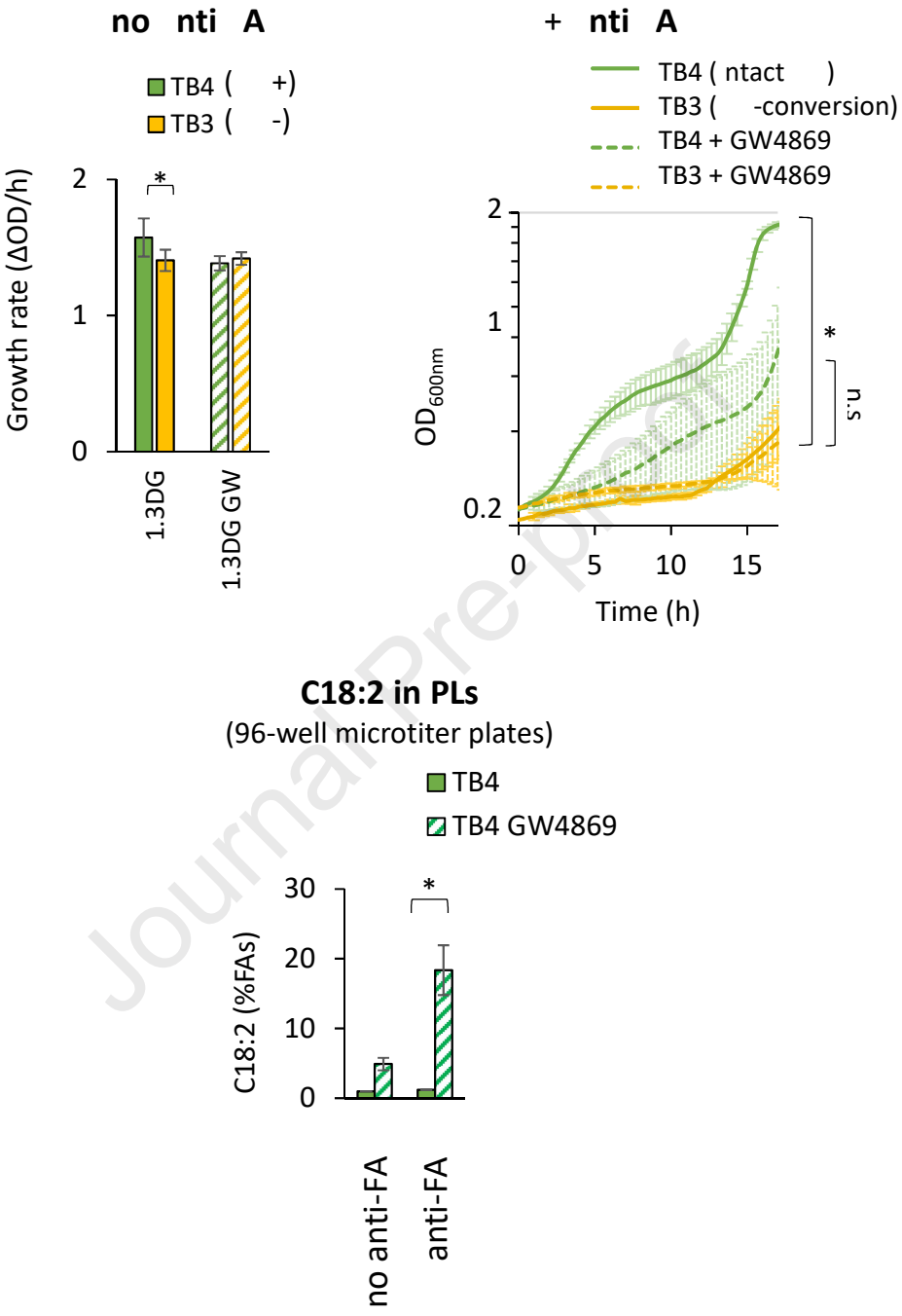
no nti A
TB4 (+)
TB3 (-)
Growth rate (ΔOD/h)
2
1
0
*
1.3DG
1.3DG GW
+ nti A
TB4 (ntact)
TB3 (-conversion)
TB4 + GW4869
TB3 + GW4869
OD600nm
2
1
0.2
0
5
10
15
Time (h)
*
n.s
C18:2 in PLs
(96-well microtiter plates)
TB4
TB4 GW4869
C18:2 (%FAs)
30
20
10
0
*
no anti-FA
anti-FA

Fig. 6

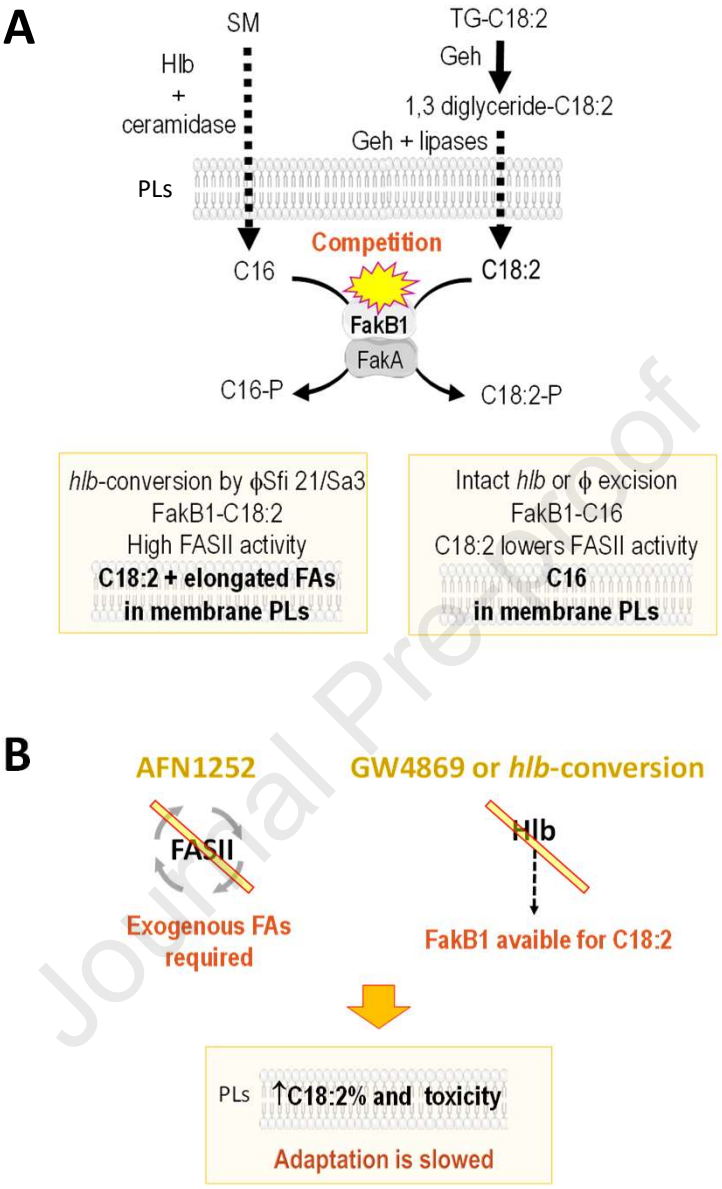

Fig. 7

Declaration of interests

☒ The authors declare that they have no known competing financial interests or personal relationships that could have appeared to influence the work reported in this paper.

☐ The author is an Editorial Board Member/Editor-in-Chief/Associate Editor/Guest Editor for *[Journal name]* and was not involved in the editorial review or the decision to publish this article.

☐ The authors declare the following financial interests/personal relationships which may be considered as potential competing interests: